Saint Petersburg State University

VICHARE Aniket Sachin

Final qualifying work

Interpretation of geomorphometric characteristics of the daytime glacier surface based on remote sensing data

Level of education: Bachelors

Speciality 05.03.03 « Cartography and Geoinformatics »

Scientific supervisor:

Professor of St Petersburg state University

Nico Giovanni

Reviewer:

Federal state budgetary institution
“All-Russian Research
Geological Institute. A.P. Karpinsky”

Candidate of geology and mineralogy

Nikolskaya Olga Andreevna

Saint Petersburg

2023

CONTENTS

LIST OF FIGURES

LIST OF TABLES

INTRODUCTION

Analysing and quantifying changes in glacier has been going for many decades. With introduction of Earth Obervation Satellites in 1960s, the scientist started using these satellites for analysis of glaciers. The geomorphological mapping plays an important role in understanding the relation between earth, hydrology and atmosphere. (Reddy, 2018)

The Snow and glaciers are one the most important factors in shaping of earth. Presently, with more important given to global warming and effects of climate change, it is well known that any changes to glacier helps us to study the effects of climate change and the consequences of it. Glacial geomorphology is the scientific study of the processes, landscapes, and landforms produced by ice sheets, valley glaciers, and other ice masses on the surface of the Earth. These processes include understanding how ice masses move, and how glacial ice erodes, transports, and deposits sediment. (Menzies, 2009)

This works helps to observse application and limitation of DInSar method for analysis of mountainous glaciers. The territory for the observation and verification of method was selected were glaciers of Altai regions: namely Potanin and Alexandra glaciers.

The remote sensing method has many benefits over traditional methods by cost effective, access to data and time frame. Since its inception, the remote sensing methods for analysis geomorphological methods has been used. The feature usually observed, analysed and quantified are such snow cover, snow texture, albedo, glacier extent, temperature changes, creation of 3D models of glaciers, glacier velocity (surface & vertical) and glacier accumulation & ablation. The remote sensing method uses satellites and UAVs (Unmanned Aerial Vehicles) for glacier analysis with the help of Optical, Radar, Thermal infrared and LiDAR sensors.

Most of the analysis of the glaciers are done in optical spectrum. The use of radar satellite images for analysis are also widely accepted.

The aim of the thesis is to:

1. Learn types of method for geomorphological method for analysing glacier
2. Fammarlize with the current remote sensing methods used for analysis of glaciers
3. Gain understanding of basic principles behind DINSar (Differential Interferometric Synthetic Aperture Radar) method.
4. Study the method for downloading SAR data.
5. Understanding the processes behind processing of data in ESA (European Space Agency) open Scientific Toolbox Exploitation Platform's (STEP) SeNtinel Application Platform (SNAP).
6. Process and analysis of remotely sensed data through the SNAP for glacier analysis.
7. Comparison of result received through UAV for evaluation of output.

For development of method for analysis of glacier, the satellite chosen was of European Space Agency's (ESA) Senitel-1A, which has open access to data. Processing of data was done in open-source toolbox of ESA's SNAP Desktop 8.0 and 9.0 program and open-source software QGIS (Quantum Geographic Information System) for visualization and final output.

The given thesis has four chapters. The first chapter looks at geomorpholocial features of glaciers and different methods for analysing, quantifying the features. Next chapter specifically see the application of remote sensing in the field of glacier monitoring. The third chapter is about the Sentinel-1 satellite and theory of Differential Interferometric Synthetic Aperture Radar (DInSAR) method. The fourth chapter is processing, application and verification of the method on example of Potanin-Alexandra Glaciers of Altai mountains. In the conlcusion, the result received were of the ablation / vertical displacement & velocity and possible application for analysis of glaciers.

CHAPTER 1 ANALYSIS OF STUDY OF GEOMORPHOLOGICAL ANALYSIS OF GLACIERS

1.1 Type of Geomorphological analysis of Glacier

Glaciers are large masses of ice that form over time from the accumulation of snow. They have a variety of geomorphological features such as Cirques, Moraines, Glacial valleys, till and crevasse.

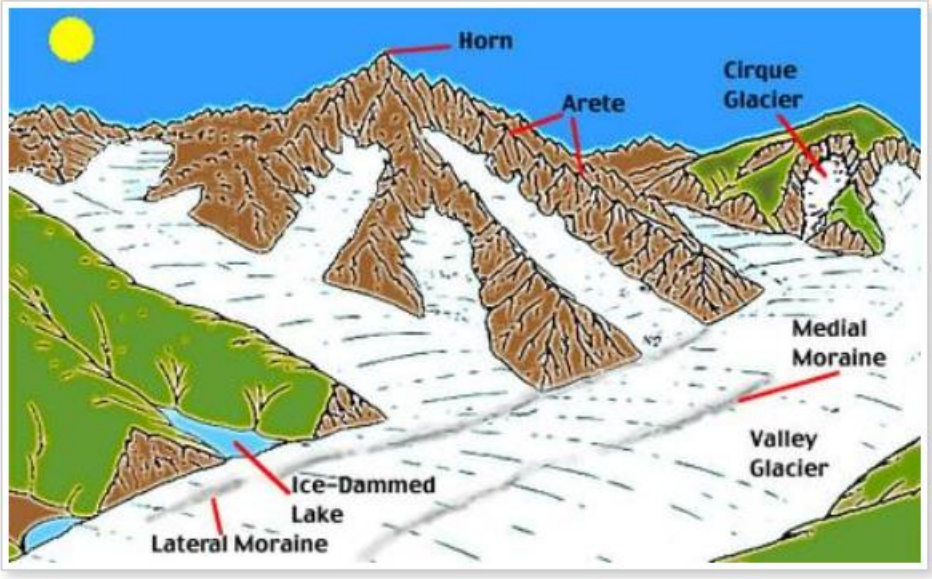

Figure 1. Glacial features (Climate Change Education, 2023)

Below are the few definitions of the glacial features from the book Fundamentals of Geomorphology by (Huggett, 2007).

Cirques: These are bowl-shaped depressions that form at the head of a glacier where snow and ice accumulate. In other words, typically armchair-shaped hollows that form in mountainous terrain.

Moraines: These are ridges of rock and debris that are carried along by the glacier and deposited at its edges.

Glacial valleys: These are U-shaped valleys that are carved out by glaciers as they move down mountain sides.

Crevasse: These are deep cracks in the ice that form as the glacier moves and stretches.

The Geomophological analysis of the glacier is the study of the processes, landscapes and landform of the valley and ice sheet glaciers. The processes which are studied are movement of glaciers, vertical and horizontal velocity, erosion processes, how sediments are transported and deposited. These features can vary depending on the size and shape of the glacier, as well as the climate and geology of the surrounding area.

These features are mostly studied by range of methods such as field observations, remote sensing techniques, geophysical surveys. These methods are studied on alone or combination of methods are used for comprehensive methods.

Field obervations usually involve visiting site of interest and making observation of the features and processses. This method is produces more detailed information on the processes and features. Mapping of glaceirs, studying glacier dynamics such as ice velocity, temperature and melt water discharge is done. Field observations are necessary as they verify and provide ground truth data that can be validated with other methods such as remote sensing. The Ground-Penetrating Radar (GPR), Geodetic Surveys and remote sensing techniques like aerial survey are done when in field.

Remote Sensing method involves using satellite or aerial imagery to study the surface features of glaciers. It can provide information on the extent, location, and changes in glaciers over time. The few methods that are used for analysis are:

- Optical Remote Sensing
- Thermal Infrared Remote Sensing
- Synthetic Aperture Radar (SAR)
- Light Detection and Ranging (LiDAR)
- Aerial Remote Sensing and Photogrammetry

Ground-Penetrating Radar (GPR) method involves sending electromagnetic waves into the ice and measuring the reflections to determine the thickness and internal structure of glaciers. This study is also called Radioglaciology (Schroeder, 2020).

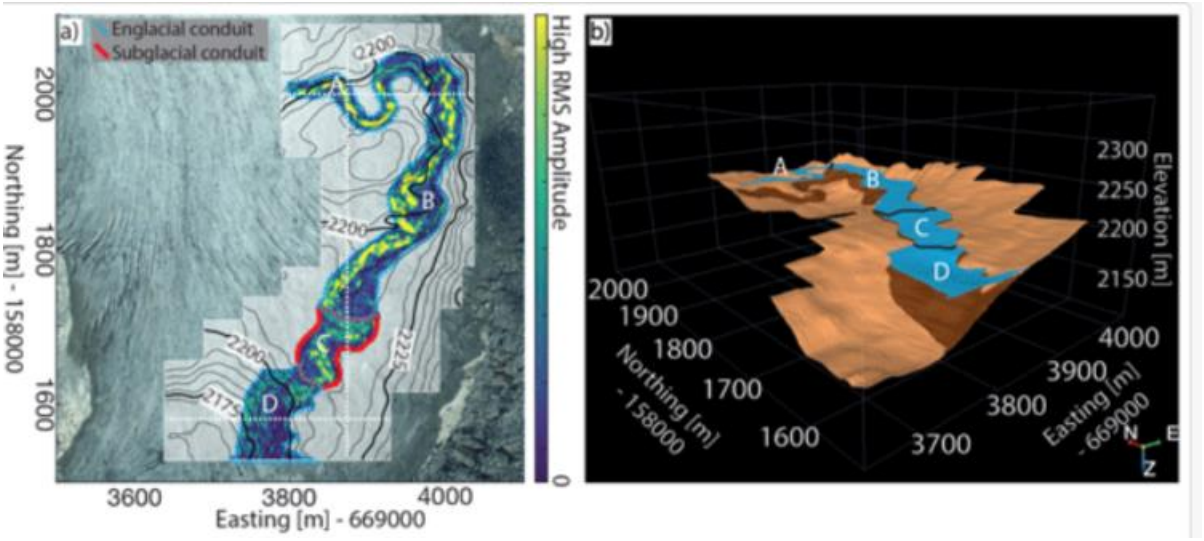

Figure 2. Subsurface drainage of Rhonegletscher glacier using GPR by (Church, 2021)

Terrestrial Laser Scanning method involves using a laser scanner to create a 3D model of the glacier surface. It can provide information on the volume and mass balance of glaciers.

GPS and Geodetic Surveys method involves measuring the movement of glaciers using GPS and other geodetic techniques. It can provide information on the velocity and direction of glacier movement. The method uses geodetic methods such Real Time Kinetic or Static GNSS survey. The method is used to create terrain model for different time period of the glaciers.

1.2 Current methods and experiences for monitoring glaciers using remote sensing

Since the first launch of Earth Observation satellite Landsat 1, scientist started using Multi Spectral Scanner (MSS) for analysing glacier. It helped to cover glaciers with big area which were not possible before. Since that many different satellites with different sensors have been launched into orbits. These satellites played very important roles for development of remote sensing methods for analysis of galciers.

Remote sensing is a commonly used method for analyzing glaciers. It involves using satellite or aerial imagery to study the surface features and changes of glaciers. The following are some of the remote sensing methods used for analysing glaciers:

Optical Remote Sensing:

This method involves using visible and infrared light to study glaciers. It can provide information on the surface texture, albedo, and snow cover of glaciers. The analysis of the glaciers is ususally done with using diffferent Spectral indices and spectral reflectance of the ice in different spectrum. The few common Spectral indices which are used:

- Normalized Difference Snow Index (NDSI)
- Snow Water Index (SWI) (Dixit A, 2019)
- Normalized Difference Water Index (NDWI)
- New Snow Index (S3) (Alvarinho J. Luis, 2020)

The (Andreas Kääb, 2015) investigated the potential of Sentinel-2 satellite imagery, also evaluated the radiometric and geometric performance of Sentinel-2 for glacier analysis.

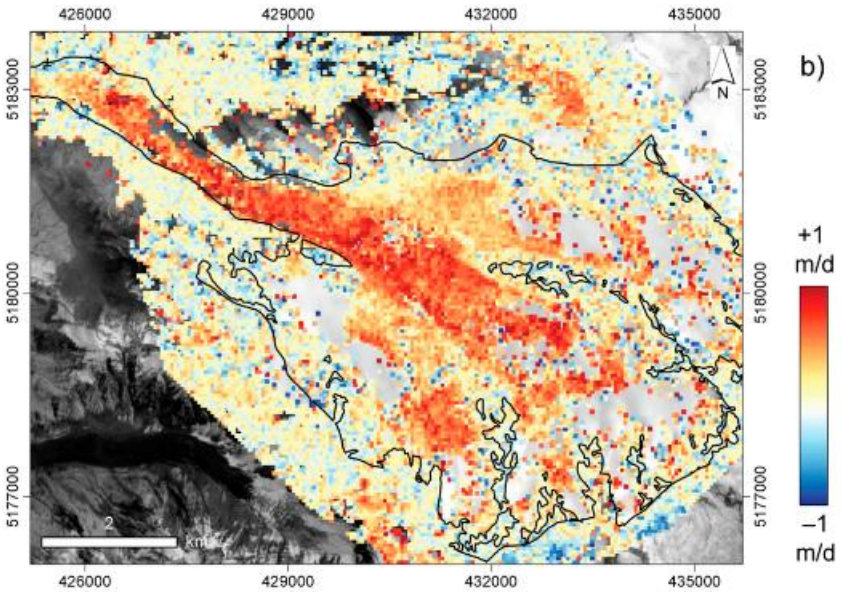

Figure 3. Ice Speed of Fox Glacier between december 2015 and january 2016 using Sentinel-2 by (Andreas Kääb, 2015)

Synthetic Aperture Radar (SAR):

SAR uses radar waves to measure the surface of glaciers. It can provide information on the extent and velocity of glaciers, as well as the presence of crevasses and other features. The method Interferometry is used for analysis of the glaciers where two images of same area using same sensor or different sensors are used. Few of the methods are Offset Tracking, DInSAR, PSI, etc.

In Microwave Spectrum range using SAR data ERS-1 and ERS-2, the analysis of mass balance and velocity of ice flow was shown by (Ian Joughin, 2001).

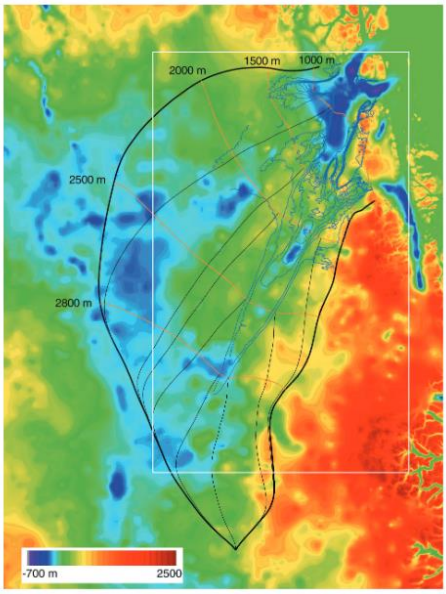

Figure 4. Ice stream speed contours of Northeast Greenland (Ian Joughin, 2001)

Light Detection and Ranging (LiDAR):

LiDAR uses laser pulses to create a 3D model of the glacier surface. It can provide information on the volume and mass balance of glaciers. The (А.В.Погорелов, 2015) used LiDAR images for Fishct glacier for monitoring of Mounatain Glaciers. They found average decrease was by 2m. Also (Adhikari, 2019) studied the changes in surface elevation and mass balance. The study highlighted the importance of LiDAR for momitoring and understanding impactof climate change.

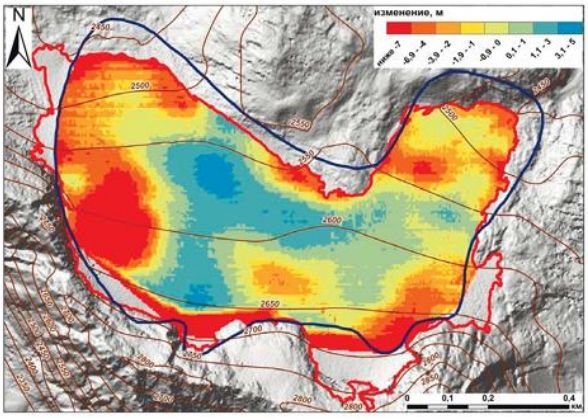

Figure 5. Ice Decrease of fisht glacier from 1982 -2010 (А.В.Погорелов, 2015)

Thermal Infrared Remote Sensing:

This method involves using thermal sensors to study the temperature of glaciers. It can provide information on the melting and refreezing of glaciers. The Glacier surface temperature could be analysis using Thermal Infrared Bands (TIR). Below image shows average temperature druing April,2019 for Zemu Glacier, India using Landsat- 8 TIR bands. (Vichare, 2021)

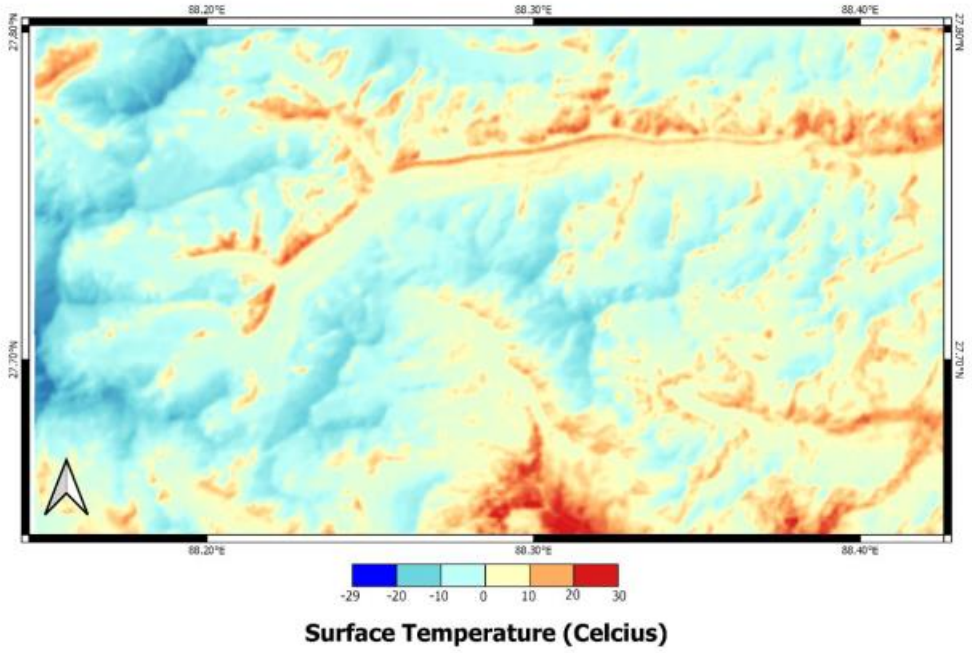

Figure 6. Surface Temperature, Zemu Glacier from LandSat-8 (Vichare, 2021)

Aerial Remote Sensing and Photogrammetry

The techique uses manned and unmanned aerial vehicle for analysis of glacier. Glacier extent, vertical and horizontal changes, snow line, glacier thickness and surface elevation. This method is cost effective than traditional method and accurate than other remote sensing methods due to high level of accuracy.

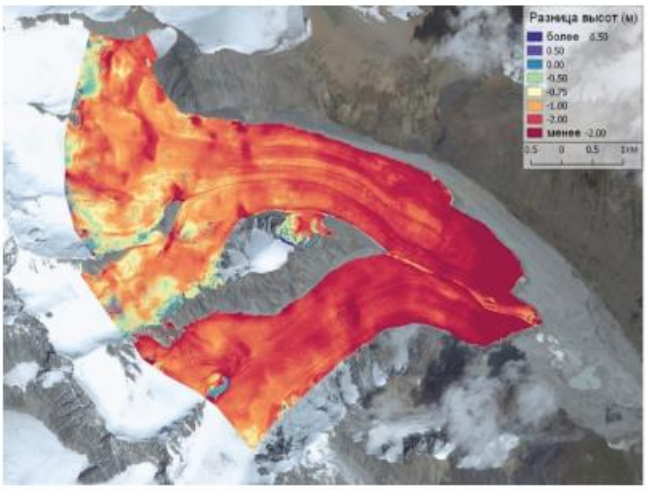

Figure 7. Height difference during ablation season of Alexandra--Potanin glacier during ablation season,2015 (Бляхарский Д.П., 2019)

CHAPTER 2 PRINCIPLES IN APPLYING RADAR TECHNIQUES INTERFEROMETRY FOR MONITORING GLACIERS

2.1 Basic principles and characteristics of radar sounding of the Earth

RADAR IMAGING

It is a type of remote sensing method carried out by a radar - an active microwave sensor capable of emitting and receiving. The radar is an active microwave sensor capable of emitting and receiving polarised radio waves scattered by the Earth's surface in specific wavelength (frequency) bands. The signal carries information about physical and geometrical properties of the object sensed.

The microwave region of the spectrum covers wavelengths from approximately 1mm to 1m. Microwaves are capable of penetrating the atmospheric features such as haze, light rain, light snow, clouds, and smoke so that microwave remote sensing is not affected by most atmospheric conditions (Microwave Remote Sensing, n.d.).

Band	Wavelength (cm)	Instrument
Ka	0.8–1.1	–
K	1.1–1.7	–
Ku	1.7–2.4	–
X	2.4–3.8	TerraSAR-X, TanDEM-X, COSMO-SkyMed
C	3.8–7.5	SIR-C, ERS 1/2, ENVISAT ASAR, RADARSAT 1/2, Sentinel-1 C-SAR
S	7.5–15	ALMAZ
L	15–30	JERS-1, SEASAT, ALOS PALSAR
P	30–100	–

Table 1. Band Wavelength of Radar Satellite with instruments

The wavelength used for the remote sensing of the earth happens to be in band X, L and C with wavelength ranging from 2 to 30 cm. as seen in the above table. The wavelength X and L are

usually used for Glacier surface analysis, due to penetration of microwave signals in L bands as seen in the figure below.

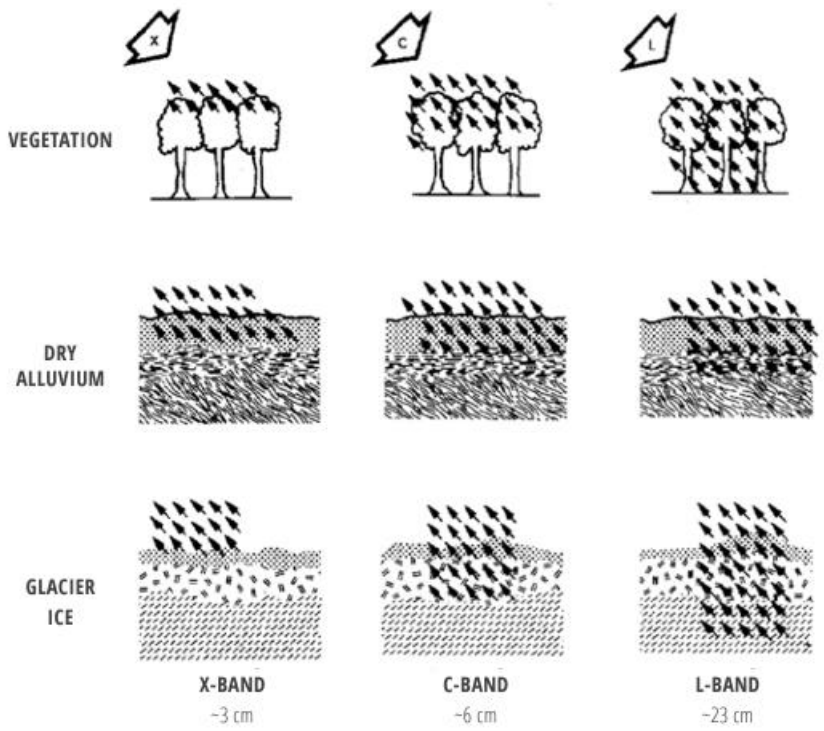

Figure 8. Signal penetration by sensor wavelength (Meyer)

Radar imaging applications include topographic mapping, geology and mining, oil spill monitoring, sea ice monitoring, oceanography, agricultural classification and assessment, land use monitoring and planetary or celestial investigations.

The first experimental use of SAR in Earth orbit was in 1978. On July 26 that year, NASA launched the satellite SEASAT. Among other instruments, it carried an L-band SAR and a wind scatterometer (PHILIPPE LACOMME, 2001). Since, its launch many more Radar Satellites have been launched into orbit. Few of them are listed below.

System	Country	Year of launch	Band	Resolution (m)
SEASAT	USA	1978	L	25
ERS 1/2	Europe	1991/1995	C	30
J-ERS	Japan	1992	L	18
SIR-C	USA	1994	L	–
X-SAR	Germany/Italy	1994	C/X	15–25
Radarsat-1/2	Canada	1995/2007	C	10–100/3–100
SRTM	USA/Germany/Italy	2000	C/X	90/30
ENVISAT	Europe	2002	CA	30, 150, 1000
ALOS	Japan	2006	L	7–100
TerraSAR-X	Germany	2007	X	1–16
TanDEM-X	Germany	2009	X	1–16
COSMOS-SkyMed	Italy	2009	X	1–100
RISAT-1	India	2012	C	3-5
ALOS-2	Japan	2014	L	10–100
SMAP	USA	2015	L	250
Gaofen	China	2016	C	1-500
PAZ	Spain	2018	X	1-15
PAKSAT	Pakistan	2018	C	-
ASNARO	JAPAN	2018	X	10
ICEYE-X1	Finland	2018	X	1-16

Table 2. Radar Satellites with bandwave

2.2 Principles of radar interferometry

Radar interferometry, also known as SAR interferometry, is a technique used to measure and analyze changes in the Earth's surface over time. It combines data from two or more synthetic aperture radar (SAR) images of the same area, taken at different times, to create an interferogram. This interferogram displays the phase difference between the two images, which can be used to extract information about the topography, deformation, and other changes on the Earth's surface.

The use of two SAR images acquired over the same area at different time or slightly different view angles togenerate maps of surface deformation or digital elevation by exploiting the differencesin the phase of the waves returning to the radar sensor is called interferometry SAR (Kenyi & Kaufmann, 2003)

The principle behind radar interferometry is based on the fact that the two SAR images being compared are affected by the same atmospheric and geometric factors, such as the satellite position and the Earth's rotation. By comparing the phase difference between the two images, it is possible to cancel out these factors and isolate the changes in the Earth's surface. The interferogram is created by combining the two images, pixel by pixel, and calculating the phase difference between them.

The synthetic aperture radar (SAR) complex single look image data delivered by ERS-1 and ERS-2, ENVISAT, TerraSAR-X, RADARSAT, ALOS and by USA Shuttle with X -SAR (DLR) can be successfully used for interferometric analysis. (Motagh, n.d.)

In synthetic aperture radar imaging, the 3D objects of the scene are mapped to the two-dimensionalazimuth-range image plane. Due to the side-looking imaging geometry and the fact that radaris based on measuring the distances to the real-world objects, certain geometrical effects occur if elevated objects are illuminated such as tree, buildings or slope of mountain (Schmitt, 2014). Because of this geometric effect such as foreshortening, layover and shadowing can happen.

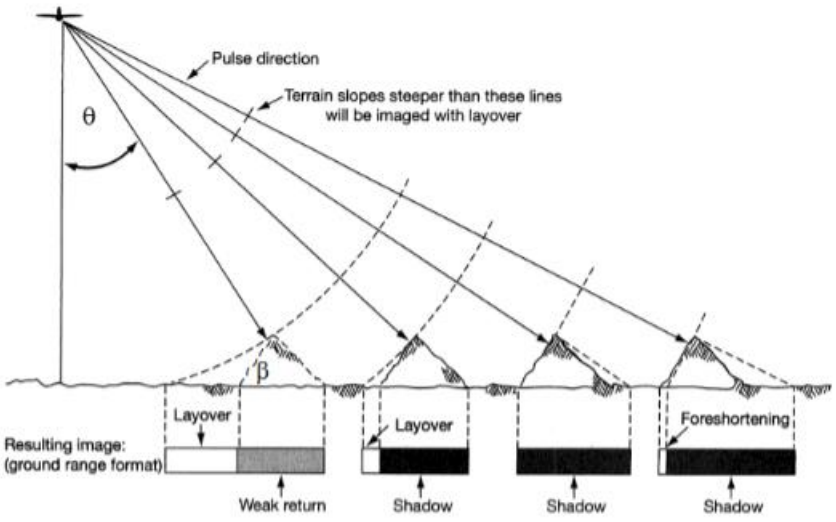

Figure 9. Geomertic effects in SAR imaging

There are different of inteferomertic method depending on the number of passes it made. If the area is captured with two different sensors, one for transmiting and other for receiving, they are called single-pass interferometry. The two images if taken from same sensor over the object is resulted in repeat pass interferometry or double pass interferometry (Hellwich, 2000)

The radar interferometry also varies according to configuration of baseline vector. They are based on the geometric configuration.

- Across-Track Interferometry
- Along Track Interferometry

Across Track Interferometry is used for measuring Topography and Deformation of the surface and Along Interferometry is used to estimate the radial velocity or motion of the target on the ground.

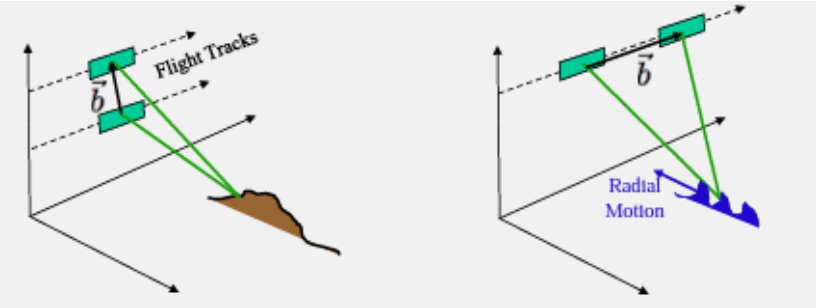

Figure 10. Interferometry radars based on configuration of baseline (Fielding).

2.3 Methods of interferometric processing for glacier analysis

There are many methods known for glacier analysis using Synthetic Aperture Radar (SAR) interferometry such as Differential Interferometry (DInSAR), Persistent Scatterer Interferometry (PSI), Small Baseline Subset (SBAS), Coherent Target Monitoring (CTM) and Tomographic SAR (TomoSAR).

Differential Interferometry (DInSAR)

Differential interferometry (also called shearing interferometry) is a method to measure derivatives of light phase distortions (A. Davaille, 2007).The basic principle behind it measures the phase difference between two SAR images taken at different times to detect surface

deformation, including glacier motion and volume changes. It consists in the comparison of the interferometric phase of two SAR radar images acquired over the same area on different dates.

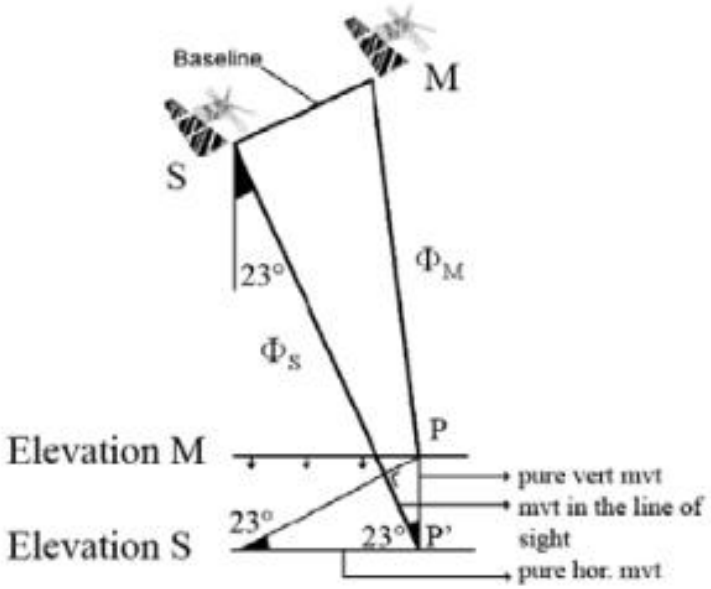

Figure 11. Principle of DinSAR (Damien Closson, 2011)

Persistent Scatterer Interferometry (PSI)

The method uses a stack of SAR images to detect the displacement of stable natural reflectors (persistent scatterers) on the glacier surface, which can then be used to estimate surface deformation. Continue here. PSI method can be used to check stabilty of geomorpholgical features such as moraines and slopes around glacial lakes. The technique uses time series of SAR images to identify persistent scatterers. It measures phase shift of the radar signal and calculate displacement of the reflectors. Thus, calculating glacier deformation, movement and velocity.

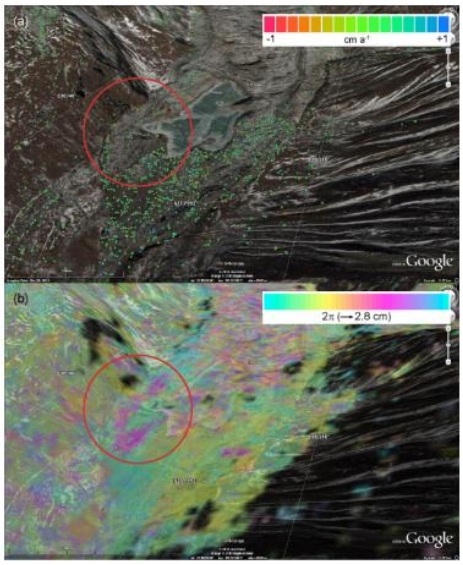

Figure 12. ice velocity by PSI velocity at glacier tongue of Thangothang Chhu glacier, Bhutan (Cristian Scapozza, 2019)

Small Baseline Subset (SBAS) method, a variant of PSI that uses a subset of images with small baselines to reduce atmospheric effects and improve accuracy. Coherent Target Monitoring (CTM) - uses a single SAR image to detect the phase changes caused by surface deformation, including glacier motion and volume changes.

Tomographic SAR (TomoSAR) - a new technique that uses multiple SAR images from different viewing angles to create a 3D image of the glacier surface and detect ice thickness changes. It was studied by (G. D. Martin-del-Campo-Becerra, 2021), to show capabilities of TomoSAR to detect the subsurface structures in alpine glaciers.

CHAPTER 3 DEVELOPING OF A METHOD FOR MONITORING MOUNTAIN GLACIERS WITH HELP SATELLITE INTERFEROMETRY BASED ON SENTINEL 1 DATA

The six satellite missions have been launched as part of the European Union's earth observation initiative Copernicus with each Sentinel mission consisting of at least 2 satellites and some, such as Sentinel 1, consisting of 4 satellites.

The Sentinel-1 and Sentinel-2 missions have the objective to monitor 5 earth biophysical and land cover qualities using both radar and high- resolution optical platforms ("ESA, Copernicus, Overview", 2014). They both have single instrument on the platform. The sentinel-1 objectives are to provide continuous radar mapping of the earth. The Sentinel-2 was launched in 2015 and 2015 was observation in optical range of spectrum. It acquires high-resloution multispectral images similar to Landsat 8 or 9. The objectives were of monitoring land, climate change and geophysical observations.

The Sentinel-3 satellites which carry 4 instruments were launched in February 2016 and April 2018 has objective of measuring sea surface topography, sea, ocean and land surface temperature to support for forecasting enviornmental and climate monitoring of oceans with high accuracy and reliabilty.

The Sentinel-4 and Sentinel-5 objectives are to monitor are quality over Europe and the World respectively. The Sentinel-6 which carries instrument Poseidon-4 is receive data about radar altimeter and a microwave radiometer.

3.1 General information about Sentinel-1 and its sensors

In the year 2014, on 3rd April ESA lauched satellite Sentinel 1A into orbit. The satellites are based on the Piattaforma Italiana Multi Applicativa (PRIMA) platform with a mission-specific payload module, in this case the CSAR (C-band Synthetic Aperture Radar) instrument. It was built by industrial consortium led by Thales Alenia Space (Italy). (Sentinel-1: ESA's Radar Observatory Mission for GMES Operational Services, 2012)

The Sentinel-1 consist of two polar-orbiting satellites performing C-band synthetic aperture radar imaging. It operates and capture data both at daytime and night. The resolution of the images would be upto 5m. As SAR wavelength is not affected by cloud cover or a lack of illumination, it can acquire data under all weather condition and during day or night time. It consists of a constellation of two satellites, Sentinel-1A and Sentinel-1B, which helps them to have short revisit time of 6 days.

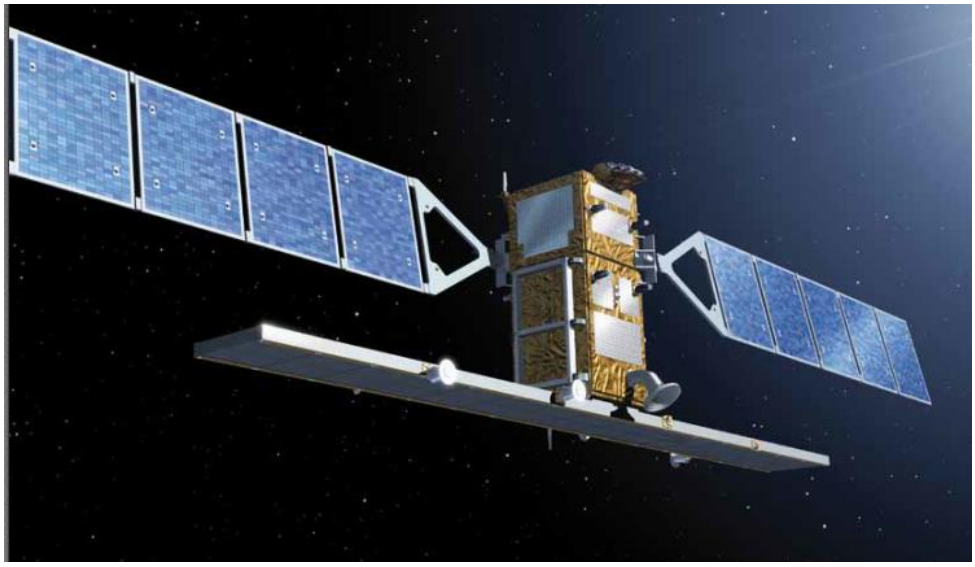

Figure 13. ESA's Sentinel-1 (Sentinel-1 User Handbook, 2016)

The payload of Sentinel-1 is C-band synthetic aperture radar instrument operating at a frequency of 5.405 GHz. The radar of the Sentinel-1 spacecraft operates in four modes, which differ in operating technology, capture bandwidth, spatial resolution obtained from images and the possibilities of shooting in different polarizations.

The product from Sentinel-1 days will used for numerous mission such as

- Monitoring and mapping of sea-ice
- Oil-spill mointoring
- Ship detection
- Mapping of land, forest surface
- Monitoring land deformation

The operational modes for sentinel-1 are:

- Interferometric Wide-swath mode (IW)
- Wave mode (WV)
- Strip Map mode (SM)
- Extra Wide-swath mode (EW)

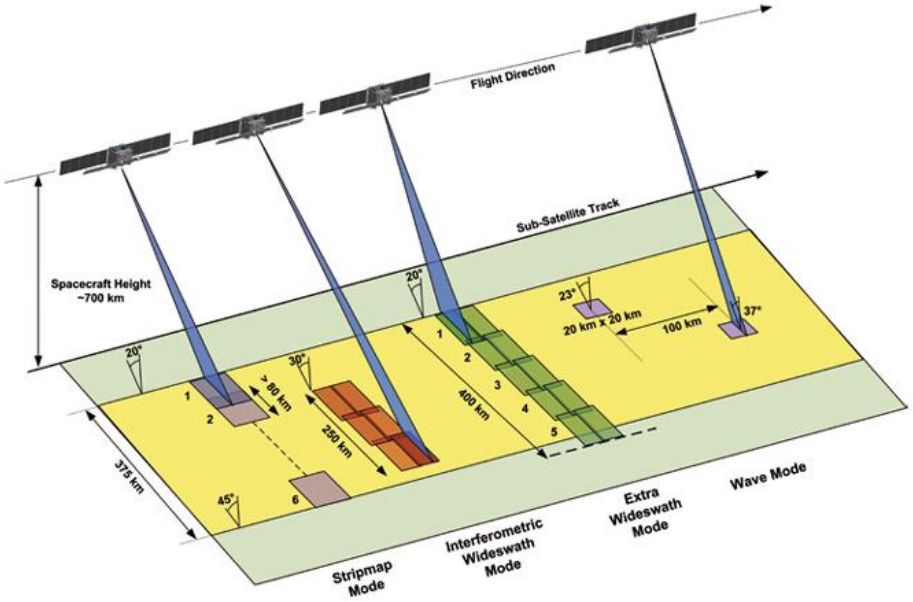

Figure 14. Sentinel 1 Operational modes (Sentinel-1: ESA's Radar Observatory Mission for GMES Operational Services, 2012)

The IW mode captures three sub-swaths using Terrain Observation with Progressive Scans SAR (TOPSAR). The EW mode also employs TOPSAR techniques but with with swath over 400 km. The WV mode uses leap frog acquistion techniques and SM mode is non continous mode with better resolution.

The table showing different type of captures mode and its parameters below

Acquistion mode	Swath wide	Incidence angles	polarization	Resolution
Interferometric Wide-swath mode (IW)	250 km	31° – 46°	Dual (HH+HV, VV+VH)	20 x 5 m
Wave mode (WV)	20 km	23° - 37°	Single (HH, VV)	5 x 5 m
Strip Map mode (SM)	80 km	20° – 47°	Dual (HH+HV, VV+VH)	5 x 5 m
Extra Wide-swath mode (EW)	410 km	20° – 47°	Dual (HH+HV, VV+VH	40 x 20 m

Table 3. Characteristics of Sentinel-1 acquistion mode

The polarization schema of all modes shown below in the fig ().

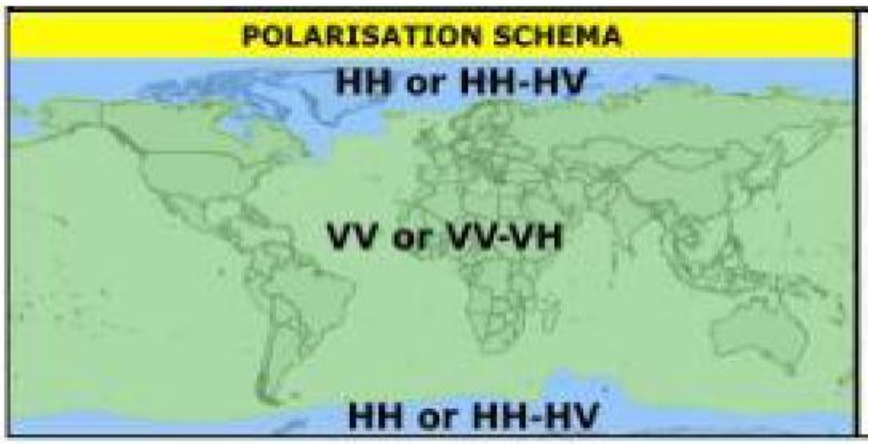

Figure 15. Polarisation Schema *("ESA, Copernicus, Overview", 2014)*

Sentinel-1 Operational Products

The Sentinel-1 products generate three levels of data. The Payload Data Ground Segment (PDGS) is responsible for exploitation of the instrument data. The PDGS usually generate data and user products and distributes in raw level-0 products. It also processes level-1 and level-2 products. (Payload Data Ground Segment (PDGS), 2016).

Level-0

The data is compressed and unfocused SAR (Synthetic Aperture Radar). Level-0 data primarily consists of noise, internal calibration, orbit, and altitude data. The data is availble to users in only SM, IW and EW mode of acquistion.

Level-1

Level-1 data is product of level-0, which is processed for generation of Single Look Complex (SLC) and Ground Range Detected (GRD) products. These products contain phase information, natural pixel spacing, detected amplitude and impact of speckle.

Single Look Complex (SLC) – This is complex radar data, i.e., containing amplitude and phase of the signal. SLC is data in single look, slant-range. It contains data about amplitude and phase information. The data of this level is used in interferometric processing to obtain information about heights and displacements of the probed surface.

Ground Range Detected (GRD) – The focused SAR data is detected, multi-looked. The ellipsoid projection of the product is projected using Earth ellipsoid model (WGS-84).

Level-2

The data is consisting of geophysical products derived from level-1. The level-2 products are Ocean Wind field (OWI), Ocean Swell spectra (OSW) and Surface Radial Velocity (RVL). The availability of components depends on the acquisition mode.

3.2 Interferometric processing by the multi-time DInSAR method

The SNAP Toolboxs were developed from early 2014 as common new toolbox for upcoming Sentinel platforms. It was created on the basis of BEAM and NEST. The SNAP core development is led and organised by Brockmann Consult as previously for BEAM and NEST. SNAP is built on 17 years of experience in EO software development and EO data processing & analysis. It was meant to have one tololbox for all the upcoming missions. Till 2015 it was only a

standalone toolbox for spaceborne SAR data (2 SNAP Introduction and News, 2019). The current version or as common SNAP for Sentinel 9 was released in 2023

The Sentinel Toolbox and the scientific data processors use a simple data input/output format, which makes it easy to import SNAP data in other imaging applications. The format is called and has been developed by SPOT-Image, France. The SNAP software uses a special DIMAP profile called BEAM-DIMAP.

In simple words, the very basic of Differential interferometry is forming of interferogram on the basis of relief model and use it to together with another interferogram to obtain differential interferogram. The interferograms are created using two images, where the first one is Master image and following one is Slave image (ШИРШОВА, 2019). The process of creating Velocity map could be done in three steps

I. Evaluation of coherence
II. Creation Differential Interferograms
III. LOS (Line of Sight) Vertical Displacement/ Velocity map

Coherence

Coherence is the complex correlation between two complex SAR images and consists phase and a magnitude component. The magnitude varies between 0 and 1, at which 0 refers to no correlation and 1 to perfect correlation (Ayman Abdel-Hamid, 2021). For Sentinel 1 images coherence is calculated by module TOPSAR Cross correlation operator in SNAP Desktop. TOPSAR techique is where data is acquired in the form of bursts, used in IW mode and EW mode of acquisition.

Figure 16. Intensity of VV polarization, Altai mountains, 17 May 2017

Since the SAR products have large extent and as it is acquired in TOPSAR method, it can be split into slices for better and fast processing of data. The first step is to split the image using TOPS Split operator.

For vertical change or difference, VV polarization (vertical transmission and vertical reception of waves) is used. It is necessary to apply orbit file as SAR products are not accurate and it should be corrected using precise orbit files. As for SNAP Desktop, it automatically finds and apply orbit files when command is run.

Next process is to do Back Geocoding, which coregisters two products and Digital Elevation model (DEM) pixel by pixel. The next step is to perform eenhanced spectral diversity/ESD is then performed in order to achieve the required azimuthal precision registration.

Interferogram is generated in next step, it is a complex image resulted from combination of master and slave image. The result is created in phase diferrence of the surface. The final step is TOPSAR Deburst, where diiferent slices are combined into one single images.

Figure 17. Coherence output for images (27.05.2017 and 06.0.6.2017)

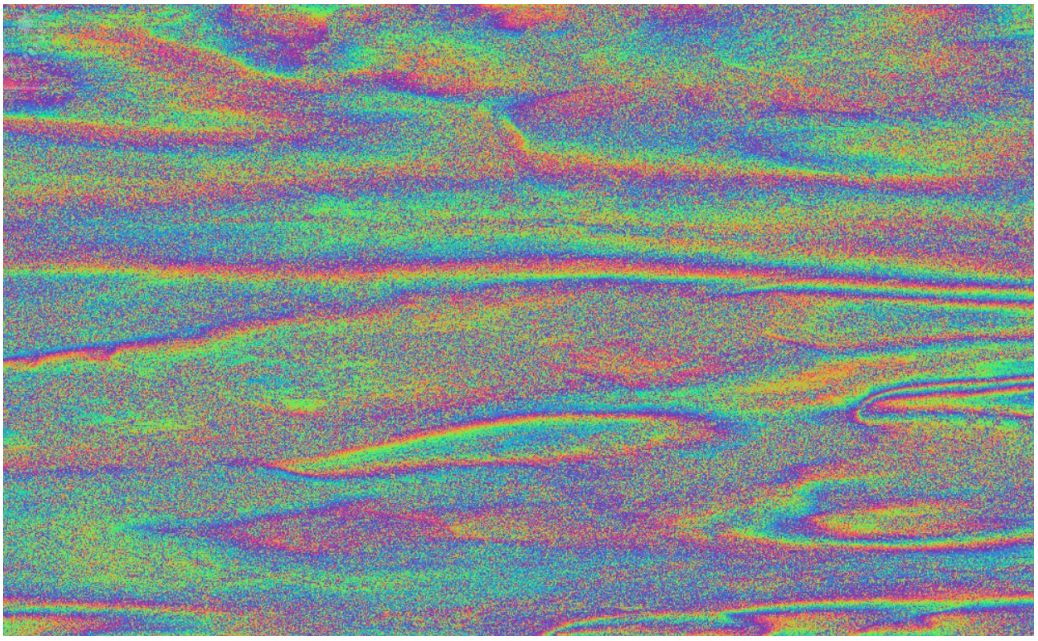

Figure 18. Interferograms generated for images (27.05.2017 and 06.0.6.2017)

As mentioned by (Ayman Abdel-Hamid, 2021), the value 1 show perfect correlation and 0 shows no correlation. More the correlation between two images, the quality of the interferogram image will be better.

Ice surfaces lose their coherence quickly, often in a matter of days. In addition, flowing ice can very quickly create a displacement gradient that exceeds interferometric capabilities (i.e., they can create more than one fringe per pixel); ice motion can also lead to a general loss of coherence (Alessandro Ferretti, 2007). The values of coherence for ice surface above 0.2 were used for creating and interpreting maps.

Creating Differential Interferogram

The interferometric phase consists of a topographic and displacement term, the processing required to separate these two components goes under the name of differential interferometric processing (Interferometric SAR Processing, 2007).After creating interferogram, it is necessary to create differential interferogram where noise and other distortion such as error due to relief and instrument error is corrected and removed.

The steps followed were to remove Topographic Phase relief, Multilook and Filtering (Goldstein filter). The Topo Phase Removal is done using Digital Elevation model (DEM), in this SRTM was used.

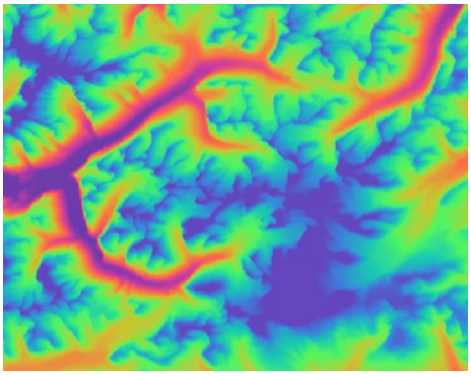

Figure 19. Topo Phase

The next step is Multilooking. The interferograms generated contains lot of noise due to

- temporal decorrelation
- Geometric decorrelation
- Volume scattering
- Processing error

It is necessary to reduce the noise by averaging adjacent pixels. (Goldstein & Werner, 1998). It can remove uncorrelated noise due temporal, baseline, volume such as due to atmospheric trubulence, errors in flattening or DEM removal.

#

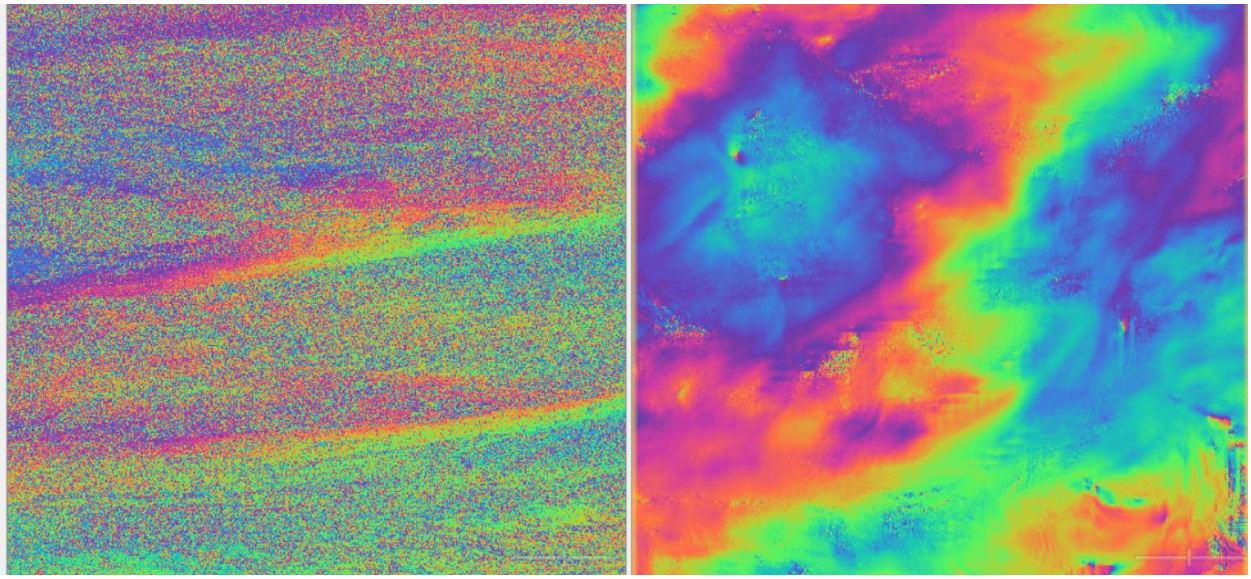

Figure 20. Before and After converting Interegram to Differential Interferogram

For the final output, the interferograms were unwrapped using Standalone tool for SNAP called SNAPHU: Statistical-Cost, Network-Flow Algorithm for Phase Unwrapping (Chen C. W., 2001) (Chen C. W., 2002). It was developed by Chen and Zebker and software is publicly available.

Its an algorithm for recovering phase data which is ambigous and known within 2π. In order to be able to relate the interferometric phase to the topographic height, the phase must first be unwrapped. (Sentinel-1 InSAR Phase Unwrapping using S1TBX and SNAPHU, 2019)

Final step was converting unwrapped phase to Displacement vector. It was done in Snap using operator Phase to Displacement. With result of the displacement is often as Line-of-Sight movement. The below figure shows the principle behind it.

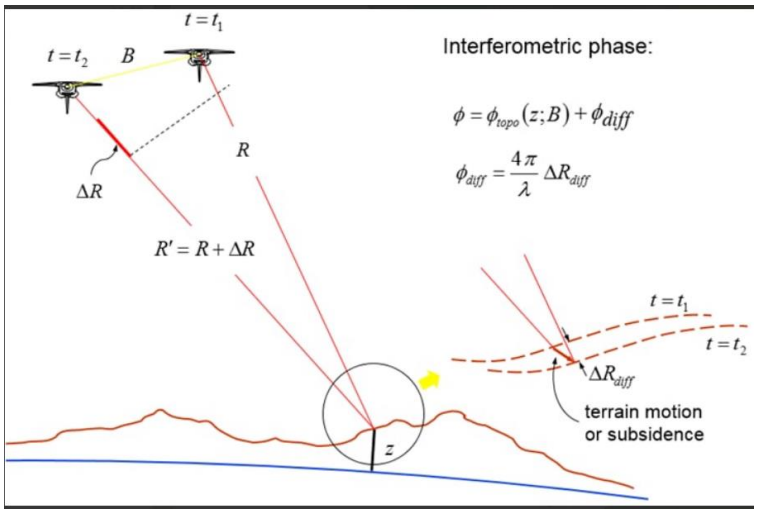

Figure 21. Basic princple of Interferometric method (DInSAR) (ШИРШОВА, 2019)

The next step is to geocode image by correcting SAR geometric distortion such as variation in scene, tilt of the sensor and also topographic variation. It was done by operator Range-Doppler Terrain Correction. The result is transformed into WGS84 coordinate system.

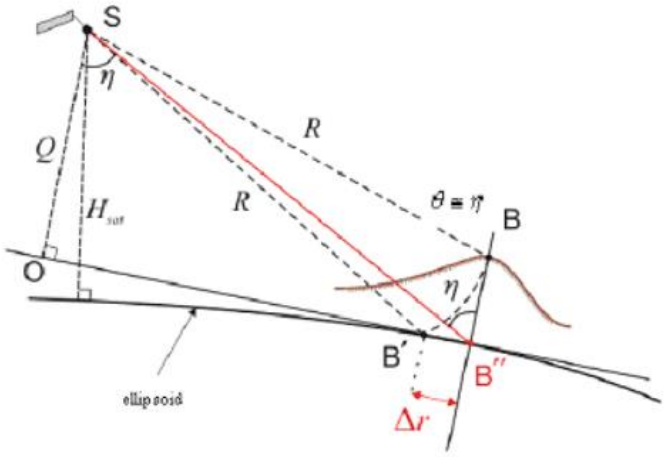

Figure 22. terrain Correction (SNAP Desktop)

All this process were using Graph Builder in SNAP Desktop. The processes were semi automatic as parameters were always needed for all pairs to be manually entered.

The visualization and calculation were done in QGIS.

CHAPTER 4: OBSERVATIONS IN METHOD FOR VERTICAL CHANGE/ABLATION IN MOUNTAIN GLACIER

The Dinsar method for glacier velocity was tried on Mongolion mountain glacier of the Tavan Bogd Range, Potanin Glacier and Alexandra Glacier. The Glaciers are located above 3000 m.

Figure 23. Ground photograph of the Potanin Glacier (right) and Alexandra Glacier (left), Tavan Range, Mongolian Altai Mountains. Khuiten Peak, at 4374 m a.s.l. the highest peak in Mongolia, is in the center in the background. From Davaa and Kadota (2009).

The Glacier extent were drawn with help of RGB composite image made from Sentinel-1 pairs for june,2015. Also, it was drawn from using sentinel-2 with spectral index of NDSI and False Colour Composite (FCC) of bands 11,8,3. They were overlayed on google earth imagery for choosing best outline possible.

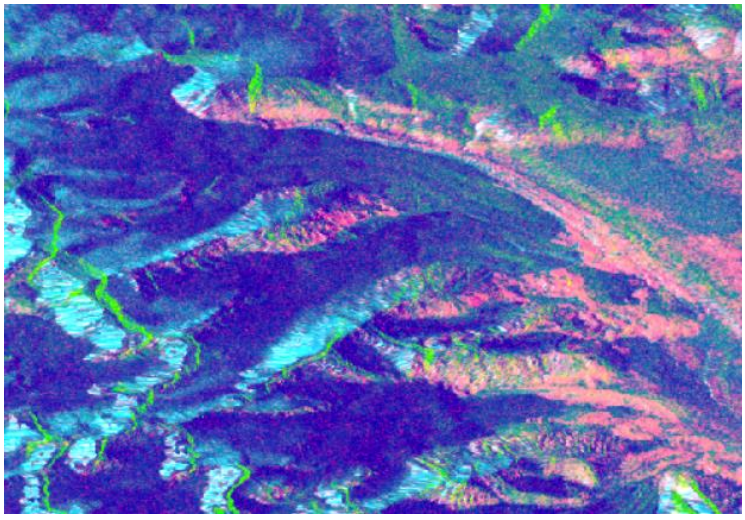

Figure 24. Rgb from sentinel-1 slc (05.06.2015 and 29.06.2015)

The RGB composite was made using two simultaneous images of Sentinel-1 SLC proposed by ESA advanced training course for sentinel-1 by (Foumalis, 2015). The red band was given Coherence of the pair, green colour was assigned to Sigma (Multilook) average of the VV polarization and blue was give difference of sigma VV polarization. The few features like moraines could be identified from the RGB composite. Retreat line of the glacier could be seen, which was zig zag in nature. Also, at the tongue of the glacier, glacial lake could be observed.

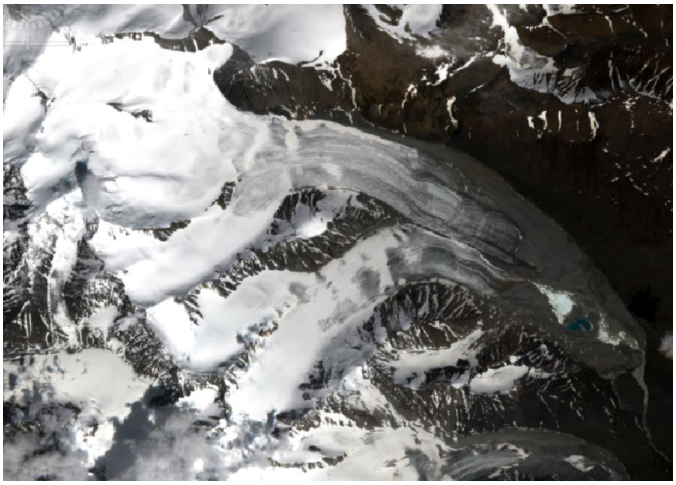

Figure 25. RGB from Sentinel-2 2015

The Sentinel-2 images were used to verify and correlate the glacier extent obtained from Sentinel-1.

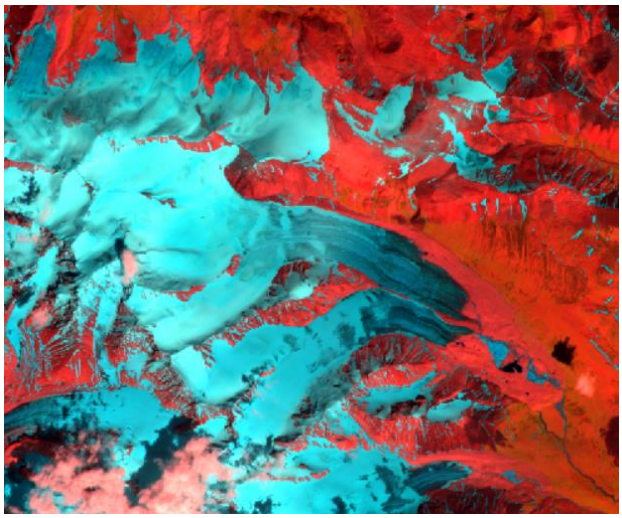

Figure 26. FCC Sentinel-2 (11,8,3 bands)

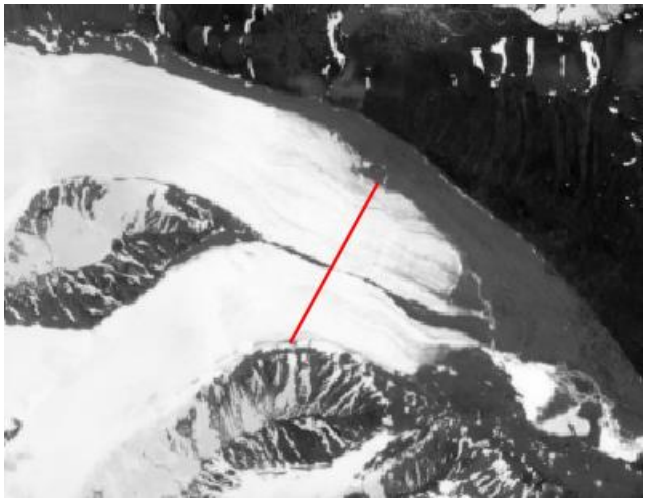

Figure 27. Cross-section of NDSI

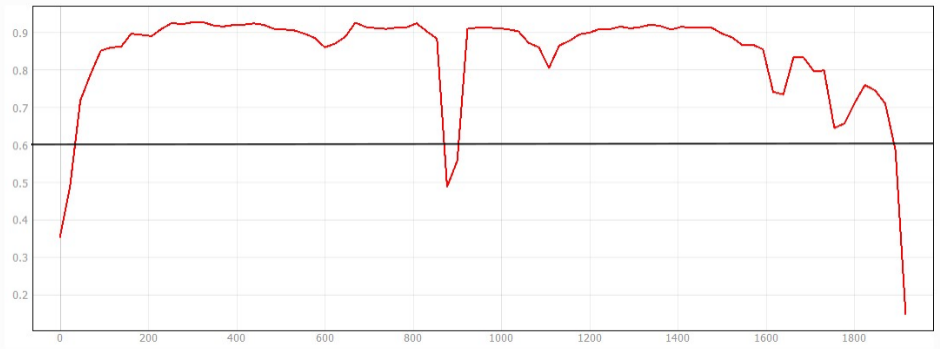

Figure 28. NDSI value on the above cross section

NDSI value showing places where moraines are, it shown by little trough on the graph and centre depression shows medial moraine between Potanin glacier and Alexandra glacier. on the cross section in figure (27),

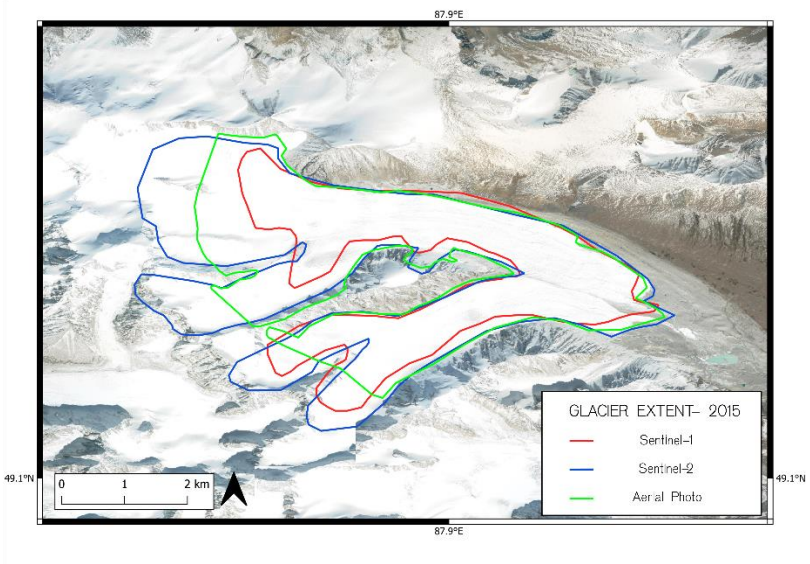

Figure 29. Comparison of Glacier extent,2015 from Sentinel-1 Sentinel-2 and (Бляхарский Д.П., 2019)

4.1 Information on Sentinel-1 images used for verification.

With open access to data from the Copernicus hub and the Alaska Satellite facility for Sentinel -1 SAR data, the satellite images of four years with continuation for the period of ablation of the glacier were dowloaded. The data from Copernicus hub and Alaska Satellite hub are exactly same with better access frim the later website.

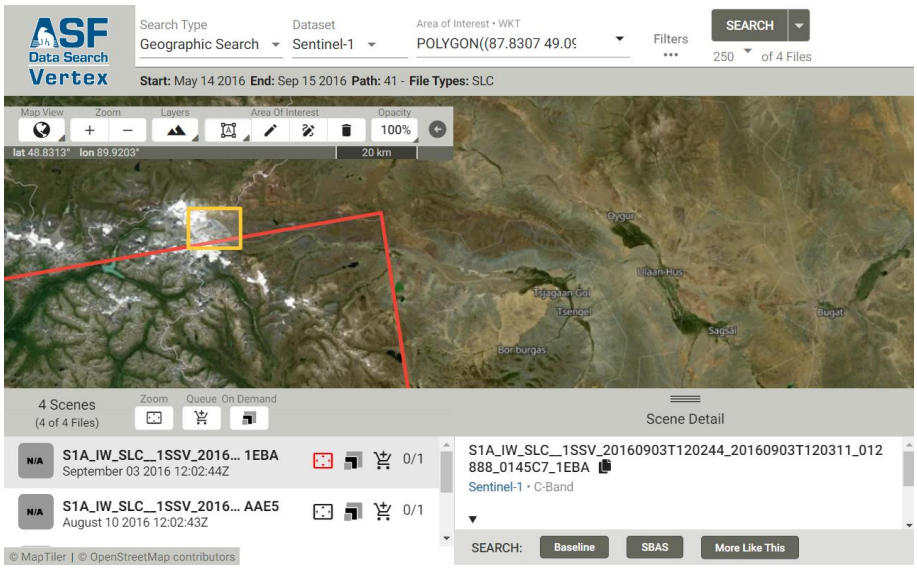

Figure 30. Overlay of available Sentinel-1 image in relative orbit 41

The period of satellite images for monitoring were from 20th may to 15th september for the year 2015, 2016, 2017 and 2018. For year 2016 no ascending pass was available in relative orbit 41 of Sentinel-1A. So, descending orbit was chosen with best territorial extent and temporal resolution possible.

Year	Master image date	No. of slave images	Last slave image date	AverageTemporal resolution
2015	06.06	4	9.09	24
2016	17.05	5	14.09	24
2017	25.05	8	10.09	12
2018	01.06	8	05.09	12

Table 4. Information of images acquired

The Orbit pass for 2015, 2017, 2018 is ascending and for 2016 is descending. The relative orbits were 41 and 143.

The type of product - SLC (Single Look Complex).

Polarization – VV (vertical transmission and vertical reception of waves)

Swath mode – IW (Intereferometric Wide Swath)

Subswath – 1 for ascending pass and 3 for descending pass

Polarsation burst – 9 & 10 for ascending and 2 & 3 for descending pass

Total Sentinel images – 29 and volume of satellite image – 147 gb.

The territory coverage of ascending pass sentinel-1 image in fig (31)

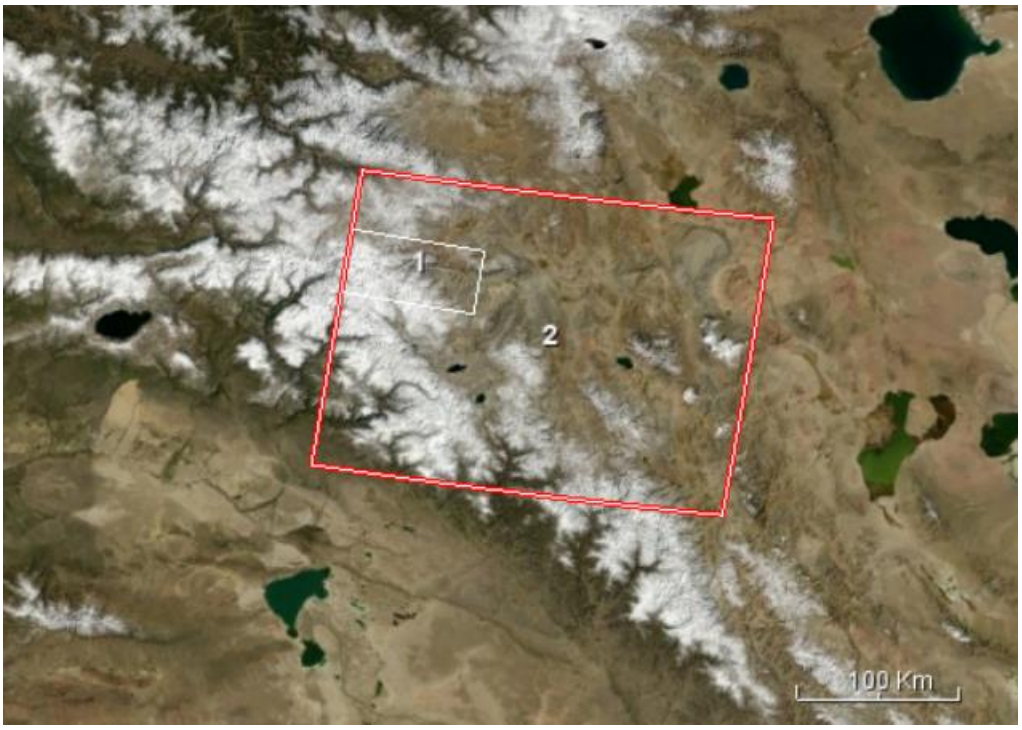

Figure 31. Territorial coverage of ascending pass

The processor

The processing of data was done on windows systems with following parameters

Processor – Intel® Core™ i7-9750H CPU @ 2.60GHz

RAM memory - 16gb

Video Graphic Card – NVIDIA GeForce GTX 1050 Ti

The process was done on open-source software SNAP Desktop. Total of 25 results were produced which were stacked by year and then visualized in QGIS.

4.2 Processing in SNAP Desktop

The Processing in the images was done in ESA's STEP programme SNAP desktop. Since the SNAP Desktop and Sentinel-1 products are both from ESA, the need of any external supporting file such as orbit file, metadata is not needed.

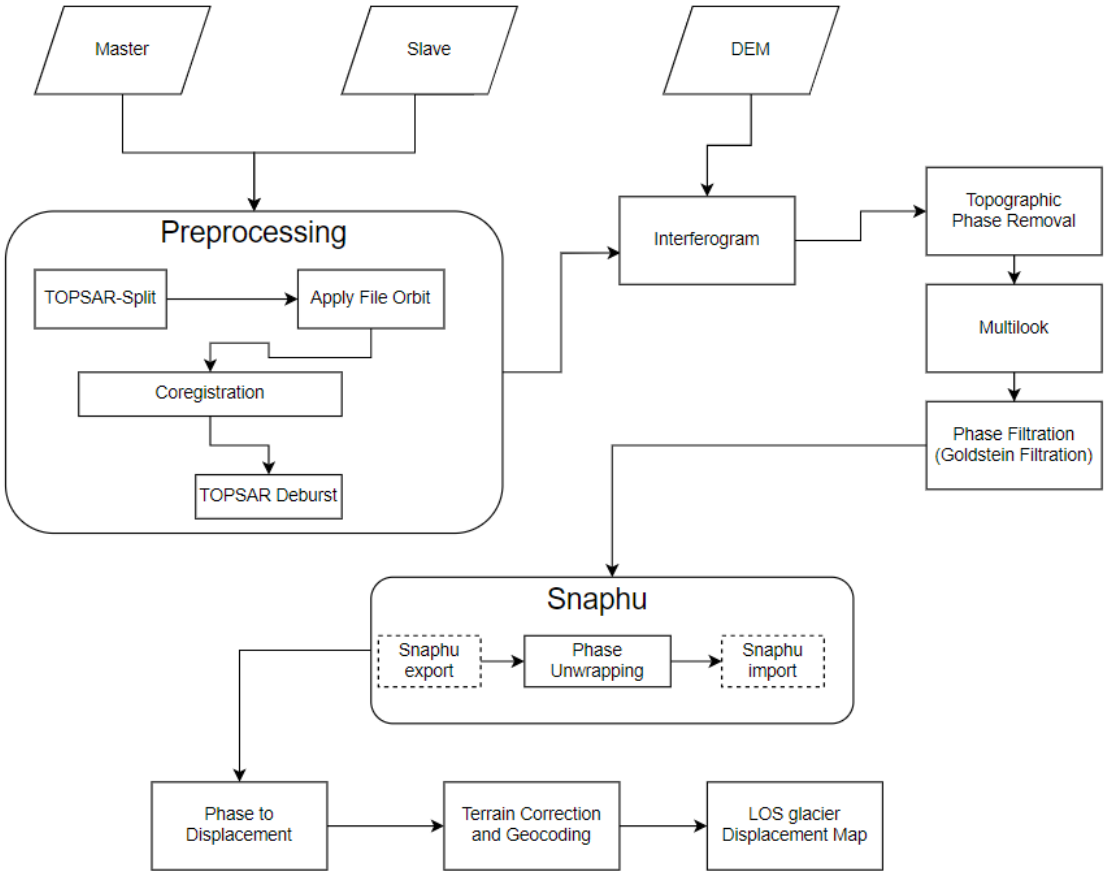

Figure 32. Preprocessing in SNAP

The Processing was done using following steps –

1. Generation of Interferogram
2. Converting it to Differential Interferogram
3. Unwrapping of product using SNAPHU
4. Convertion of unwrapped phase to displacement vector

5. Geocoding of the product
6. Stacking of the product and Visualization of the results

The average process time was for every pair of InSAR processing took on average 30 mins with most time for the SNAPHU process.

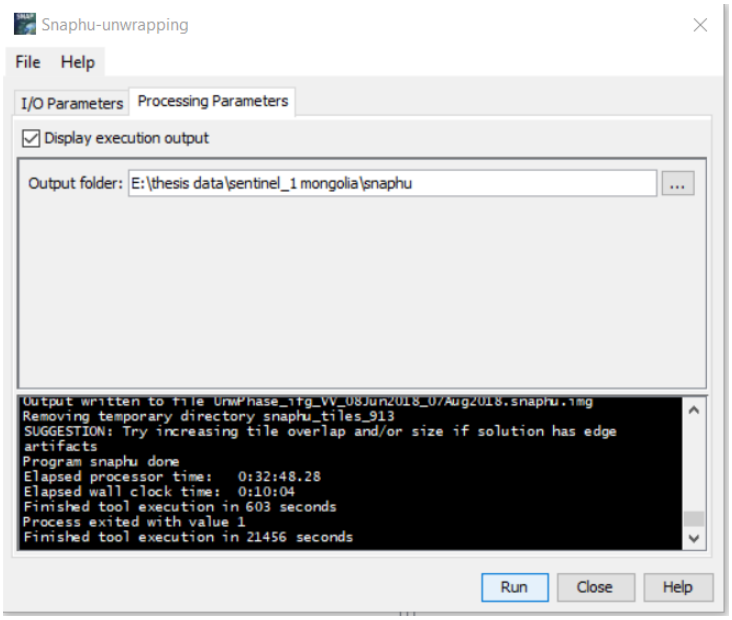

Figure 33. SNAPHU Processing - Unwrapping phase

4.3 Analysis of the result of the processed data

Four maps were generated for height difference to see decrease in different year. On that basis, vertical velocity map was created for combine 4 years.

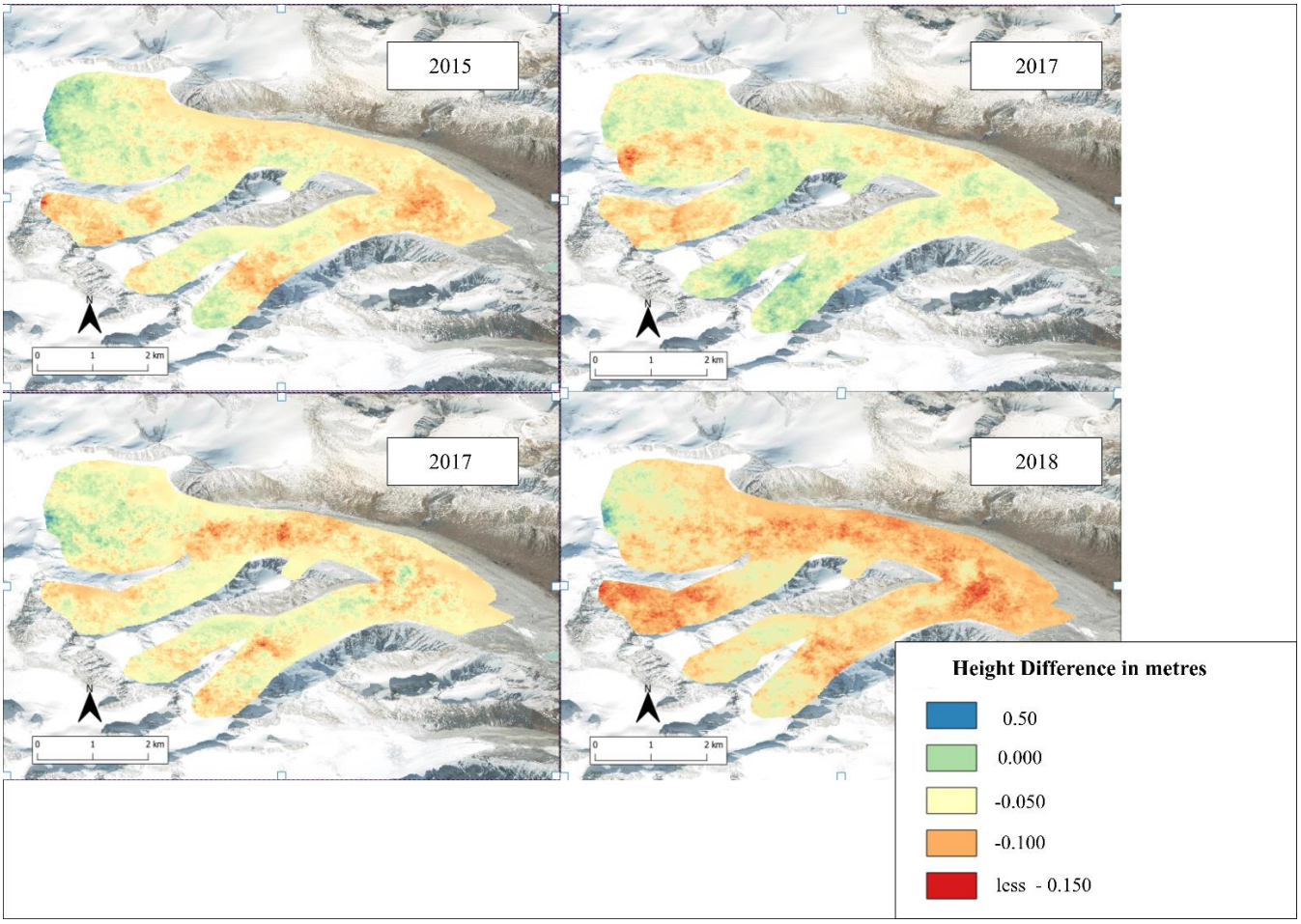

Figure 34. Vertical displacement from year 2015 to 2018 during ablation period (May to September)

The vertical velocity of the glacier for four years from 2015 to 2018 was found by combining the vertical displacement and calculating it.

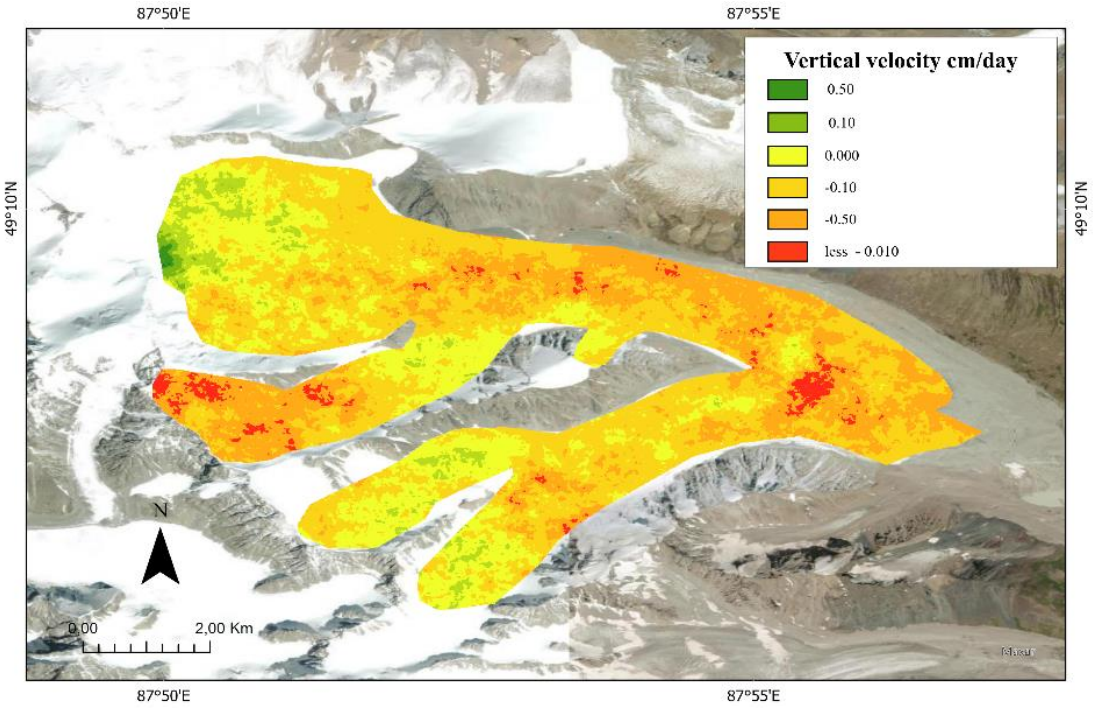

Figure 35. Vertical velocity druing ablation period (2015-2018)

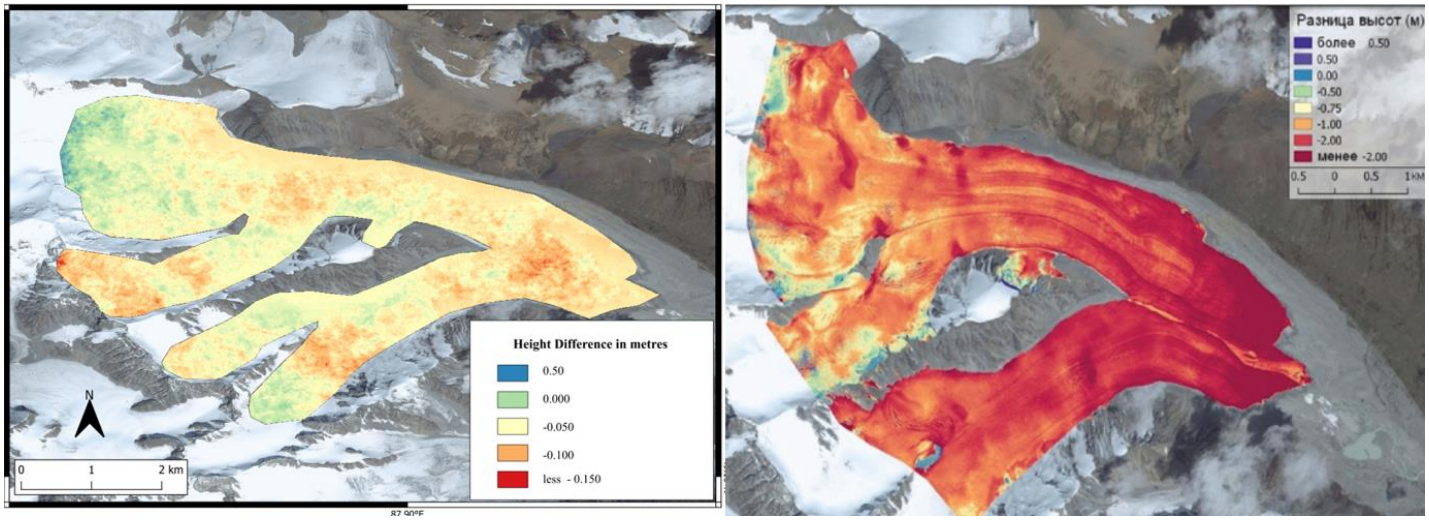

Figure 36. Height diiference (m) in 2015 ablation period. On left, results from Sentinel-1 and on right, results from 2015 expedition of (Бляхарский Д.П., 2019)

The observation made from comparing both results show approximately similar signs of changes in height differences. At the tongue of the glacier, there was less -0.15 metres in Sentinel-

1 and around -0.2 metres from UAS Surveying done by (Бляхарский,2019) results. Also, at the accumulation zone of the glacier, a positive difference was noted in both the results. This infers that DInSAR, method show good results but with less accuracy which could be attributed to the resolution of the Sentinel-1 CSAR instrument and coherence loss of ice, which is important for generation of phase difference.

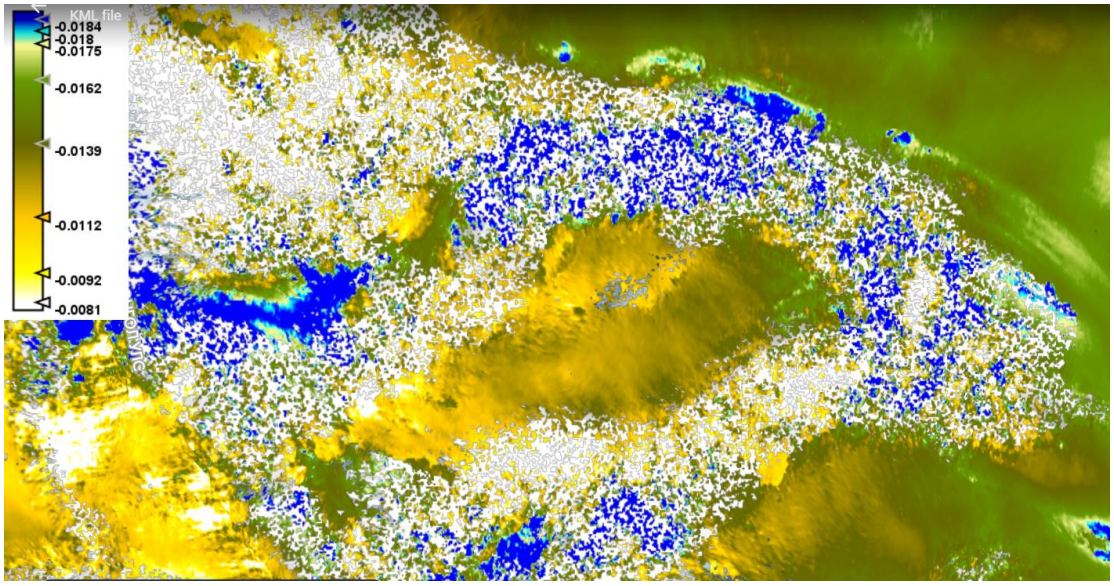

Figure 37. Vertical changes in glaciers (metres) with coherence more than 0.2

Figures (35) shows vertical change in glacier with coherence more than 0.2. The white spots show areas in the glacier surface losing it coherence value. This were interpolated in QGIS to fill the gap in between.

4.4 DInSAR limitation in analysis of mountain glaciers

DInSAR method have few limitations which affects the quality and application of the method in few stituation.

Since the mountains have steep slope and complex topography, it can lead signal loss and blockage, and also shadowing in the radar data, leading to data loss and gaps and reduced accuracy. It could be seen in figure (29) where glacier extent of Sentinel-1 is shifted little towards north as

compare to sentinel-2 and aerial photography, as it was an ascending pass orbit for 2015, from south to north, possibly due to shadowing of the data behind southern slope.

Another limitation is related to temporal decoloration which are more pronounced in alpice glaciers due to their faster flow rates and dynamic behaviour as mentioned earlier by (Alessandro Ferretti, 2007) that ice quickly loses it coherence value. It becomes difficult to detect small changes in the glacier movement. Also, the presence of snow on the glacier can cause scattering and reduce the coherence. This error is corrected by creating time series for DinSAR method for increasing accuracy and reducing error by atmospheric condition.

There could be error in Digital Model Elevation (DEM) which affects the quality of results. The SRTM data has low accuracy in mountainous region, with vertical accuracy/resolution of SRTM in mountainous topography is more than 10m. for higher elevations as studied by (Berthier E, 2006) This can lead to inaccuracies in the measurement and affect the reliability of the results.

CONCLUSION

The analysis of glacier is very important and necessary aspect for understanding the climate changes. With changes in technology every day, the Radar satellites holds very important place in remote sensing methods for analysis of geomorphological features of glaciers. The thesis proposes use of Differential interferometry method for analysis of glacier, depending on the requirement. With this a large area extent can be covered with significantly less amount of money and time required by traditional methods. This method can work comprehensively with other data to improve the accuracy for monitoring geomorphological analysis of glaciers.

In general, the following results were obtained

- The types of Geomorphological methods were seen and learned.
- Different remote sensing technique were learned and considered.
- The basic theory of radar satellite has been studied.
- Sentinel-1 data products and uses were learned.
- Semi-automation of Process was done using Graph builder in ESA's SNAP.
- The use of Differential interferometry synthetic aperture radar technique (DInSAR) for analysis of glacier were seen, and based on free Sentinel-1 data and SNAP software, methology was proposed.
- Limitation of the process were are studied.
- Verification of the results using the provided methology with available data.

In the end, the process is useful for monitoring glaciers and should be looked further into betterment of process.

ACKNOWLEDGMENTS

I am entirely grateful for the mentorship from my advisor. I Would like to thank ESA for free access to Sentinel-1 data and its open-source toolbox SNAP Desktop. Also, Special thanks to my teachers from department of Cartography and Geoinformatics, SpbU, Natalia Pozdnyakova amd Dmitriy Bliakharskii for valuable guidance and their knowledge. Thank you to Prof. Dmitry A. Ganyushkin for his time and input. I am also, grateful to Shirshova Vera from MSU, Moscow for lecture on Radar Satellite Interferometry and tips on intetrepting the results. Final thanks to my friends and family for support throughout the thesis.

LIST OF REFERENCES

1."ESA, Copernicus, Overview". (2014). Retrieved 2023, from ESA: https://www.esa.int/Applications/Observing_the_Earth/Copernicus/Europe_s_Copernicus_programme

2. SNAP Introduction and News. (2019, September 10). Retrieved 2022-2023, from STEP - Scientific Toolbox Exploitation Platform: http://step.esa.int/docs/presentations/SNAP_User_Forum/2_SNAP_Introduction%20and%20News.pdf

3.A. Davaille, A. L. (2007). 7.03 Laboratory Studies of Mantle Convection. In Treatise on Geophysics (Vol. 7, pp. 89-165). France. Doi:https://doi.org/10.1016/B978-044452748-6.00116-4

4. Adhikari, S. A. (2019). Airborne Lidar reveals spatial and temporal patterns of surface elevation and mass changes of Canadian glaciers over the past decade. The Cryosphere.

5. Alessandro Ferretti, A. M.-G. (2007). Insar Principles: Guidelines for SAR Interferometry Processing and Interpretation. (K. Fletcher, Ed.) Noordwijk, The Netherlands.

6. Alvarinho J. Luis, S. S. (2020). High-resolution multispectral mapping facies on glacier surface in the Arctic using worldview-3 data. CZECH POLAR REPORTS .

7. Andreas Kääb, F. P. (2015). Glacier remote sensing using Sentinel-2. Part I: Radiometric and geometric performance, and application to ice velocity. Remote Sensing.

8. Ayman Abdel-Hamid, O. D. (2021). He potential of sentinel-1 insar coherence for grasslands monitoring in Eastern Cape, South Africa. International Journal of Applied Earth Observation and Geoinformation, 98. Doi:https://doi.org/10.1016/j.jag.2021.102306.

9. Berthier E, Y. A. (2006). Biases of SRTM in high-mountain areas: Implications for the monitoring of glacier volume changes. Geophysical Research Letters, 33(8). Doi:https://doi.org/10.1029/2006GL025862

10. Chen, C. W. (2001). Two-dimensional phase unwrapping with use of statistical models for cost functions in nonlinear optimization. Journal of the Optical Society of America A-Optics Image Science and Vision, 18(2), 338-551.

11. Chen, C. W. (2002). Phase unwrapping for large SAR interferograms: Statistical segmentation and generalized network models. IEEE Transactions on Geoscience and Remote Sensing, 1709-1719.

12. Church, G. B. (2021). Ground-penetrating radar imaging reveals glacier's drainage network in 3D. The Cryosphere. Doi:https://doi.org/10.5194/tc-15-3975-2021

13. Climate Change Education. (2023, April). Retrieved from Camel:

Https://camelclimatechange.org/138471

14. Cristian Scapozza, C. A. (2019). Glacial lake outburst flood hazard assessment bysatellite Earth observation in the Himalayas(Chomolhari area, Bhutan). Geogr. Helv, 125-139.

15. Damien Closson, N. A. (2011). Salt Tectonics of the Lisan Diapir Revealed by Synthetic Aperture Radar Images. In Tectonics (pp. 303-311).

16. Dixit A, G. A. (2019, November 25). Development and Evaluation of a New “Snow Water Index (SWI)” for Accurate Snow Cover Delineation. Remote Sensing. Doi: https://doi.org/10.3390/rs11232774

17. Fielding, E. (n.d.). Introduction to SAR Interferometry. Applied Remote Sensing Training. Retrieved 2023, from https://appliedsciences.nasa.gov/sites/default/files/Session4-SAR-English_0.pdf

18. Foumalis, M. (2015, September). Sentinel-1 Toolbox RGB Composite for Land Cover/Use Monitoring. Bucharest, Romania. Retrieved from https://eo4society.esa.int/wp-content/uploads/2021/02/d5p1a_LTC2015_Foumelis.pdf

19. G. D. Martin-del-Campo-Becerra, A. B.-O. (2021). Subsurface tomosar imaging of the Mittelbergferner glacier in the Austrian Alps. 13th European Conference on Synthetic Aperture Radar, (pp. 1-6).

20. Goldstein, R. M., & Werner, C. (1998, November 1). Radar interferogram filtering for geophysical applications. Geophysical Research Letters, 25(21), 4035-4038. Doi:0.1029/1998GL900033

21. Guang Liu, H. G. (2016). Modified four-pass differential SAR interferometry for estimating mountain glacier surface velocity fields,. Remote Sensing Letters, 7(1), 1-10. Doi:https://doi.org/10.1080/2150704X.2015.1094588

22. Hellwich, O. (2000). Basic Principles and Current Issues of SAR Interferometry. Retrieved from https://www.researchgate.net/publication/2610545_Basic_Principles_and_Current_Issues_of_SAR_Interferometry

23. Huggett, R. J. (2007). FUNDAMENTALS OF GEOMORPHOLOGY (2nd ed.). USA.

24. Ian Joughin, M. F. (2001, december 27). Observation and analysis of ice flow in the large Greenland ice stream. Journal of Geophysical Research Atmospheres, 106, 34,021–34,034. Doi:10.1029/2001JD900087

25 Interferometric SAR Processing. (2007). GAMMA Remote Sensing.

26. Kenyi, L. W., & Kaufmann, V. (2003). Estimation of rock glacier surface deformation using SAR interferometry data. IEEE Transactions on Geoscience and Remote Sensing, 1512-1515. Doi:10.1109/TGRS.2003.811996

27. Menzies, J. (2009). Glacial Geomorphology. In Encyclopedia of Paleoclimatology and Ancient Environments. Encyclopedia of Earth Sciences Series. Springer, Dordrech (pp. 361-374). Dordrecht: Springer . Doi:https://doi.org/10.1007/978-1-4020-4411-3_92

28. Meyer, f. (n.d.). CHAPTER 2 Spaceborne Synthetic Aperture Radar: Principles, Data Access, and Basic Processing Techniques. In THE SAR HANDBOOK .

29. Microwave Remote Sensing. (n.d.). Retrieved 2023, from Introduction to Remote Sensing (ebook): https://gaview.org/drupal893/10-radar

30. Motagh, M. (n.d.). Introduction SAR Interferometry. Retrieved April 2023, from GFZ German Research Centre for Geosciences: https://www.gfz-potsdam.de/en/section/remote-sensing-and-geoinformatics/topics/radar-remote-sensing/introduction-sar-interferometry

31. Payload Data Ground Segment (PDGS). (2016). Retrieved May 2023, from About Sentinel Online: https://sentinels.copernicus.eu/web/sentinel/missions/sentinel-1/ground-segment/core-ground-segment/pdgs

32. Philippe Lacomme, j.-p. H.-c. (2001). Synthetic aperture radar. In air and apaceborne radar systems (pp. 233-264).

33. Reddy, G. (2018). Remote Sensing and GIS for Geomorphological Mapping. In G. S. Reddy, Geospatial Technologies in Land Resources Mapping, Monitoring and Management. Geotechnologies and the Environment (Vol. 21, pp. 223-252). Cham: Springer. Doi:https://doi.org/10.1007/978-3-319-78711-4_12

34. Schmitt, M. (2014). Reconstruction of urban surface models from multi-aspect and multi-baseline interferometric SAR.

35. Schroeder, D. B. (2020). Five decades of radioglaciology. Annals of Glaciology, 61(81). Doi:https://doi.org/10.1017/aog.2020.11

36. Sentinel-1 insar Phase Unwrapping using S1TBX and SNAPHU. (2019, July 11). Retrieved from Alaska Satellite Facility - Distributed Active Archive Center: https://asf.alaska.edu/how-to/data-recipes/phase-unwrap-an-interferogram/

37. Sentinel-1: ESA's Radar Observatory Mission for GMES Operational Services. (2012). ESA Communications.

38. А.в.погорелов, к. (2015). Мониторинг горного ледника средствами воздушного лазерного сканирования (на примере ледника фишт,западный кавказ). Proceedings of the international conference (intercarto. Intergis), 21. Retrieved from https://doi.org/10.24057/2414-9179-2015-1-21-247-254

39. Бляхарский Д.П., В. Н. (2019). Мониторинг ледников в сезон абляции с использованием беспилотных аэрофотосъемочных систем на примере ледников Потанина и

Александры (массив Табын-Богдо-Ола, Монголия). Изв. Вузов «Геодезия и аэрофотосъемка», 168-179. Doi:0.30533/0536-101X-2019-63-2-168-179.

40. Ширшова, в. Ю. (2019). Мониторинг оседания земной поверхности в урбанизированных районах с помощью спутниковой радиолокационной интерферометрии.

Electronic resources

41. https://sentinel.esa.int/web/sentinel/user-guides/sentinel-1-sar - SENTINEL-1 SAR User Guide Introduction

42. https://sentinel.esa.int/web/sentinel/home — Sentinel Missions

43. https://www.copernicus.eu/en — Copernicus Programme

44. https://scihub.copernicus.eu/dhus/#/home — Copernicus Open Access Hub

45. http://step.esa.int/main/download/ — Sentinel Toolboxes

46. https://web.stanford.edu/group/radar/softwareandlinks/sw/snaphu/ — Snaphu

47. https://www.esa.int/esapub/tm/tm19/TM-19_ptA.pdf -Ferretti A, et al., InSAR Principles: Guidelines for SAR Interferometry Processing and Interpretation

48. https://search.asf.alaska.edu/#/ - ASF Data Search

Course work

49. Vichare, A. (2021). Comparing Satellite imagery for Glacier remote sensing Landsat-8, Sentinel-2 and IRS Liss-3. 2nd Year Course Work.

APPENDIX 1.
SENTINEL-1 INSAR PROCESSING IN SNAP DESKTOP

Model-1

Model-2

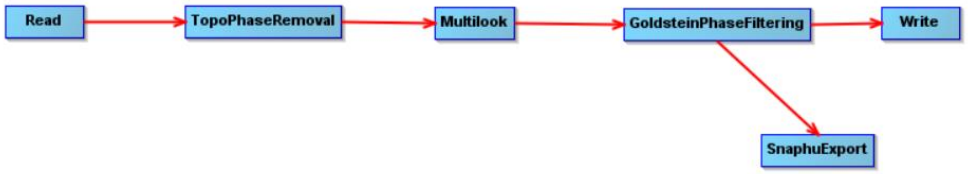

Model-3

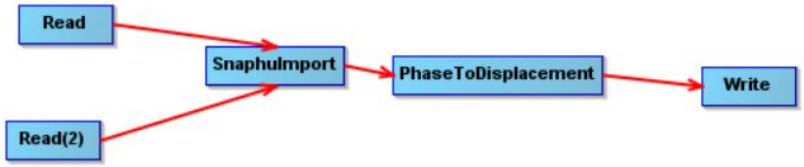

APPENDIX-2

Year	Date	Name	Orbit	Baseline (m)	Temporal (days)	Pass
2015	6.06	S1A_IW_SLC__1SSV_20150605T120236_20150605T120309_006238_00827A_62AB	41	0	0	ascending
2015	29.06	S1A_IW_SLC__1SSV_20150629T120237_20150629T120305_006588_008C64_DBAB	41	-35	24	ascending
2015	23.07	S1A_IW_SLC__1SSV_20150723T120238_20150723T120306_006938_009634_928F	41	-79	48	ascending
2015	16.08	S1A_IW_SLC__1SSV_20150816T120240_20150816T120307_007288_009FDE_AAA2	41	34	72	ascending
2015	9.09	S1A_IW_SLC__1SSV_20150909T120240_20150909T120308_007638_00A96B_7F68	41	-33	96	ascending
2016	17.05	S1A_IW_SLC__1SSV_20160517T001318_20160517T001348_011291_0111BF_56F6	143	0	0	descending
2016	10.06	S1A_IW_SLC__1SSV_20160610T001320_20160610T001349_011641_011CF9_67DE	143	-6	24	descending
2016	4.07	S1A_IW_SLC__1SDV_20160704T001327_20160704T001354_011991_012811_4203	143	127	48	descending
2016	28.07	S1A_IW_SLC__1SSV_20160728T001322_20160728T001352_012341_013381_6B8A	143	-91	72	descending
2016	21.08	S1A_IW_SLC__1SSV_20160821T001324_20160821T001353_012691_013F23_6540	143	79	96	descending
2016	14.09	S1A_IW_SLC__1SSV_20160914T001325_20160914T001354_013041_014AA7_5BBD	143	32	120	descending
2017	25.05	S1A_IW_SLC__1SDV_20170525T120251_20170525T120320_016738_01BCCB_D180	41	0	0	ascending
2017	6.06	S1A_IW_SLC__1SDV_20170606T120252_20170606T120321_016913_01C243_11DB	41	-58	12	ascending
2017	18.06	S1A_IW_SLC__1SDV_20170618T120253_20170618T120321_017088_01C7A5_7D27	41	0	24	ascending
2017	30.06	S1A_IW_SLC__1SDV_20170630T120253_20170630T120322_017263_01CCEB_9427	41	-76	36	ascending
2017	12.07	S1A_IW_SLC__1SDV_20170712T120254_20170712T120323_017438_01D23A_2E89	41	-11	48	ascending
2017	24.07	S1A_IW_SLC__1SDV_20170724T120255_20170724T120323_017613_01D78A_3374	41	11	60	ascending
2017	17.08	S1A_IW_SLC__1SDV_20170817T120256_20170817T120325_017963_01E230_B71D	41	-96	84	ascending
2017	29.08	S1A_IW_SLC__1SDV_20170829T120256_20170829T120325_018138_01E77F_99ED	41	0	96	ascending
2017	10.09	S1A_IW_SLC__1SDV_20170910T120257_20170910T120326_018313_01ECE2_698F	41	-45	120	ascending
2018	1.06	S1A_IW_SLC__1SDV_20180601T120258_20180601T120327_022163_026599_C490	41	0	0	ascending
2018	13.06	S1A_IW_SLC__1SDV_20180613T120259_20180613T120328_022338_026B08_F82E	41	18	12	ascending
2018	25.06	S1A_IW_SLC__1SDV_20180625T120259_20180625T120328_022513_027038_9BF6	41	5	24	ascending
2018	7.07	S1A_IW_SLC__1SDV_20180707T120300_20180707T120329_022688_027551_52EA	41	-24	36	ascending
2018	19.07	S1A_IW_SLC__1SDV_20180719T120301_20180719T120330_022863_027AAD_58E0	41	-93	48	ascending
2018	31.07	S1A_IW_SLC__1SDV_20180731T120301_20180731T120330_023038_028037_9DCC	41	-4	60	ascending
2018	12.08	S1A_IW_SLC__1SDV_20180812T120302_20180812T120331_023213_0285CA_6467	41	46	72	ascending

2018	24.08	S1A_IW_SLC__1SDV_20180824T120303_20180824T120332_023388_028B6C_0389	41	-12	84	ascending
2018	5.09	S1A_IW_SLC__1SDV_20180905T120303_20180905T120332_023563_029104_F024	41	-113	96	ascending